FULL-RCMA: A High Utilization EPON

Chuan Heng Foh, *Member, IEEE*, Lachlan Andrew, *Member, IEEE*, Elaine Wong, *Member, IEEE*, and Moshe Zukerman, *Senior Member, IEEE*

***Abstract*—This paper proposes an alternate solution for Ethernet passive optical networks. Our solution uses a novel protocol named full utilization local loop request contention multiple-access protocol to efficiently provide communications in passive optical networks. We study the physical layer implementation, as well as medium access control (MAC) layer protocol performance to illustrate the feasibility and benefit of our solution. The performance studies show that the MAC protocol is capable of offering 95% channel utilization under heavy load conditions. The performance results also indicate that delivery of multimedia traffic with a high quality-of-service can be achieved with our solution.**

***Index Terms*—Ethernet passive optical networks (EPONs), multiple-access communication.**

I. Introduction

TRADITIONALLY, access networks have been the most costly part of the network. This has been accentuated by the Internet. Nowadays, the cost per bit in the access network far exceeds the cost per bit in the high-capacity core networks. Moreover, the access network is lagging behind in its available capacity compared with the core network on one hand and local area networks (LANs) on the other. The currently available broadband access solutions, digital subscriber line, and cable modem networks, cannot provide many of the bandwidth hungry multimedia broadband services and applications that are available on LANs. This problem of shortage of access capacity (and with it, excessive cost per bit) is known as the *last mile problem* or the *first mile problem* depending on one's point of view.

A technology that has been considered to have the potential to solve the last mile problem successfully is the passive optical network (PON). PON is considered an attractive solution because it provides the high bandwidth associated with optic fiber, but has no active components between the customer premises and the exchange, which means significant cost reduction. There has been some interest in asynchronous transfer mode (ATM) PON [1], but the majority of research has focused on Ethernet PON (EPON) [2]–[9].

The standardization of EPON is being undertaken by the IEEE 802.3ah committee [3]. The EPON is envisaged as a reliable high bit-rate point-to-multipoint optical access network. It will provide a wide range of services to end users. It will be able to meet the capacity requirements of new multimedia services and it will be cost effective.

Traditionally, time-division multiplexing (TDM) has been used in EPONs to regulate the access of upstream traffic from the users' optical network units (ONUs) to the optical line terminal (OLT). The OLT is connected to the Internet. Although this architecture has many benefits such as scalability and the efficient use of one wavelength for many upstream channels, it leads to certain inefficiencies due to underutilized time slots [3], [5]. The recently proposed interleaved polling with adaptive cycle time (IPACT) protocol [3] uses dynamic bandwidth allocation which improves the performance. However, there is still wasted capacity in IPACT related to the polling algorithm, for example, due to unnecessary signaling traffic when an ONU is idle. The leading IEEE 802.3ah medium access control (MAC) proposal, called the multipoint control protocol (MPCP) [4], is based on IPACT. Other protocols enhancing IPACT are being proposed [6]–[9], focusing on prioritization between flows, rather than improving the aggregate throughput.

In this paper, we present an alternative MAC protocol that avoids the wastage of capacity associated with the operation of TDM and/or polling protocols. In particular, we extend the request contention multiple access (RCMA) [10] MAC to suit upstream traffic in an EPON access network. The extended protocol, full utilization local loop RCMA (FULL-RCMA) features a short access delay under light load and efficient behavior under heavy load, similar to time-division multiple access (TDMA) of the active users. It also has a very simple priority mechanism, allowing service differentiation, and does not require a complex initialization procedure. Moreover, it achieves this without centralized control. Instead, it uses the synchronizing effect of passing all data through a common passive optical splitter. This allows time to be divided into separate request and data periods, each with its own method of avoiding collisions of packets.

The remainder of this paper is organized as follows. Section II describes the FULL-RCMA EPON network architecture and protocol in detail. Section III addresses the modeling and performance analysis of FULL-RCMA. Section IV studies the performance under several traffic models with computer simulation.

Manuscript received June 30, 2003; revised January 30, 2004. This work was supported in part by the Australian Research Council. This paper was presented in part at the Optical Fiber Conference, Atlanta, GA, March 2003.

C. H. Foh is with the Centre for Multimedia and Network Technology, School of Computer Engineering, Nanyang Technological University, Singapore (e-mail: aschfoh@ntu.edu.sg).

L. Andrew and M. Zukerman are with the ARC Special Research Center for Ultra-Broadband Information Networks Department of Electrical and Electronic Engineering, University of Melbourne, Victoria 3010, Australia (e-mail: lha@ee.mu.oz.au; mzu@ee.mu.oz.au).

E. Wong is with the Photonics Research Laboratory, Australian Photonics Cooperative Research Centre, Department of Electrical and Electronic Engineering, University of Melbourne, Victoria 3010, Australia (e-mail: elw@ee.mu.oz.au).

Digital Object Identifier 10.1109/JSAC.2004.830459

0733-8716/04$20.00 © 2004 IEEE

Authorized licensed use limited to: SWINBURNE UNIV OF TECHNOLOGY. Downloaded on January 8, 2009 at 01:52 from IEEE Xplore. Restrictions apply.

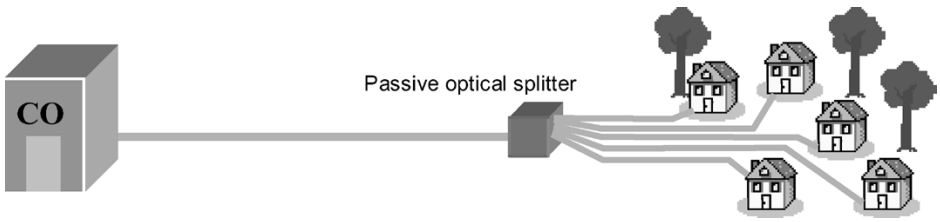

Fig. 1. Network architecture of an Ethernet passive optical network.

II. FULL-RCMA EPON

A. Overview

A fiber to the home/building (FTTH/FTTB) EPON solution optically connects a central office (CO) to ONUs in individual houses or buildings. An OLT in the CO is connected by a long fiber to a passive optical splitter near the ONUs. The splitter connects to the ONUs by short runs of fiber (see Fig. 1). This avoids using unreliable active components away from the network edges.

Data transmitted over the point-to-multipoint connection from the OLT to ONUs can simply be broadcast by the OLT. Each ONU identifies its packets by the MAC address and privacy is maintained by scrambling users' data.

The multipoint-to-point upstream connection from ONUs to the OLT can suffer contention. FULL-RCMA can relieve this. FULL-RCMA requires that the splitter echo upstream data back to all ONUs, including the sender. This requires two fibers per ONU, as depicted in Fig. 2(a), since the transmitted and echoed data use the same wavelength. This is expected to increase the cost by less than 0.3% [11]. The returned signals provide a method for senders to detect collisions of their transmissions. This is the key to FULL-RCMA. Collisions occur at the OLT if and only if they occur at the splitter. Thus, by scheduling data transmissions not to collide at the splitter, data collisions can be eliminated.

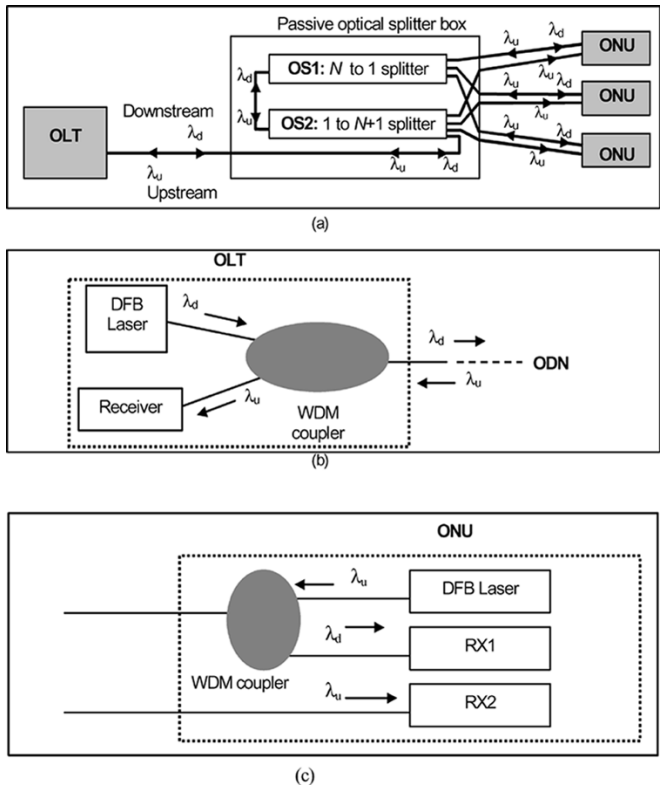

Fig. 2. (a) Network architecture of FULL-RCMA. (b) OLT transceiver. (c) ONU transceiver.

B. Physical Layer Implementation

This section outlines the physical layer requirements to implement a single-fiber 1-Gb/s EPON with a transmission range of at least 20 km and a split ratio (OLT:ONUs) of 1:16. The proposals for both components and parameters closely follow the baseline technical proposals adopted by the IEEE 802.3ah committee [12]. The baseline specifies the required functions, parameters, and parameter values for the transceivers at the OLT and ONUs, and the optical distribution network (ODN). Through the process of standardization, it is envisioned that low-cost EPON systems can be implemented through mass-producing common hardware, thus increasing the level of competition and interoperability among vendors [2].

In this paper, we consider an EPON that supports downstream and upstream transmission through wavelength division multiplexing (WDM). Two distinct lasing wavelength regions of 1480–1550 nm and 1270–1310 nm are used for downstream and upstream transmission, respectively. These regions coincide with the low-attenuation passband of a single-mode optical fiber (SMF). The large channel spacing between the downstream wavelength λ_d and upstream wavelength λ_u provides a cost-effective approach as this alleviates the need for wavelength stabilization and, hence, the need for lasers to be temperature-controlled. This, in turn, allows low-cost uncooled lasers to be used in both the OLT and ONUs.

The integrated OLT transceiver, shown in Fig. 2(b), consists of a distributed feedback (DFB) laser, a PIN-based receiver and a WDM coupler. The WDM coupler interfaces the optical transmission fiber and the OLT, specifically passing frames on λ_d from the DFB to the ODN, and frames on λ_u from the ODN to the receiver. We consider the use of a wavelength-dependent WDM coupler to improve optical link budget performance since it couples all light into one of its two arms based on the input wavelength. That is, all frames on λ_u are coupled into the output arm that is connected to the receiver at the OLT. In comparison, a 50:50 coupler halves the optical power into the two output arms irrespective of the input wavelength. As such, half of the optical power of all upstream frames on λ_u is also coupled into the output arm connected to the DFB laser, the transmitter of the OLT. This, in turn, necessitates the implementation of an isolator that prevents frames on λ_u from reaching the DFB laser,

Authorized licensed use limited to: SWINBURNE UNIV OF TECHNOLOGY. Downloaded on January 8, 2009 at 01:52 from IEEE Xplore. Restrictions apply.

and ensures the propagation of light is only in one direction, i.e., from the DFB laser to the ODN.

The ODN is the outside plant that provides all-optical transmission between the OLT and the ONUs. It consists of a SMF transmission medium and passive devices such as connectors, splices and optical splitters. A 20 km distribution link connects the OLT and the splitter unit. The splitter unit, shown in detail in Fig. 2(a), is a key component in the FULL-RCMA network architecture, consisting of an $(N+1) \times N$ optical splitter. In our case, $N = 16$. The unit broadcasts signals on λ_d, whilst providing optical loopback of a portion of the upstream signal on λ_u from each ONU to the other ONUs to facilitate FULL-RCMA. For example, in the downstream direction, the optical power of the signal on λ_d is split evenly over N output ports and is broadcast to each ONU. Likewise, in the upstream direction, the optical power of a signal on λ_u entering the splitter unit from any input port will be split amongst $(N+1)$ output ports. One output port is connected to the OLT. To facilitate FULL-RCMA, the signals emerging from the remaining N output ports are redirected back to the N ONUs, including the source ONU. The returned signals are used for monitoring collisions and scheduling transmissions amongst the ONUs.

Fig. 2(c) shows an integrated ONU comprising a DFB laser, two PIN-based receivers, namely, RX1 and RX2, and a WDM coupler. For transmission in the $\lambda_u = 1310$ nm wavelength region, we consider the use of a DFB laser in favor of a Fabry–Perot laser due to its higher bandwidth-distance product [13]. The WDM coupler optically connects the DFB laser and RX1 to OS1, while RX2 is directly connected to OS2.

The analysis in Section III of this paper is based on a distance of 1 km from the splitter unit to each ONU. However, in practice, the ONUs may not necessarily be at equal distance away from the splitter unit. Due to different optical signal attenuation paths, the optical power received at the OLT and at RX2 of each ONU may vary from frame to frame, depending on the source ONU. To overcome this problem and the fact that there are periods of inactivity on the upstream channel, burst mode capability is required at RX2 of each ONU, as well as in the receiver at the OLT. The performance analysis in this paper uses a guard time of 1 μs for threshold level recovery and clock recovery, at the "loose" end of the spectrum being considered by the IEEE committee [14], [15]. However, burst mode receivers, operating at 1 Gb/s with a capability of resetting in less than 20 ns, have been reported [13], [16]. Faster threshold levels and clock recovery times ensure minimal guard times and overheads, allowing channel efficiency to be maximized. To relax the requirements on the threshold level recovery time, the output power of each ONU can be preadjusted such that it is equalized to those from other ONUs at the splitter unit and, hence, at the OLT and RX2 [2].

Further, it is preferred that between transmissions, the DBF laser at each ONU be turned off or biased below threshold at a level such that its optical output is minimal. The spontaneous emission noise from an inactive ONU situated near the splitter unit can mask the frames transmitted from an ONU that is situated further away. At present, the specified maximum launched optical power during periods of inactivity is -39 dBm [12]. However, the laser must be able to shut down and, in turn, stabilize quickly after turning on to avoid additional overhead penalty. At the time of writing, the maximum turn on and turn off delays are yet to be specified by the IEEE committee [12]. In this paper, it is assumed that both delays are negligible.

TABLE I
OPTICAL LINK BUDGET ANALYSIS FOR A FULL-RCMA EPON WITH A DISTRIBUTION LINK OF 20 km AND A 1:16 SPLIT RATIO. THE DISTANCE BETWEEN EACH ONU AND THE SPLITTER UNIT IS 1 km

	Downstream	Upstream
Min. launch power (dBm)	1 (OLT)	-3 (ONU)
Fiber attenuation (dB)	4.2 (0.2 dB/km)	8.4 (0.4 dB/km)
Connectors, including WDM coupler (dB)	1.8	1.8
Optical splitter (dB)	15	15
Optical penalty (dB)	1	1
Power budget	22	26.2
Minimum receiver sensitivity (dBm)	-21 (RX1 @ ONU)	-29.2 (OLT)

The optical link budget analyzes for downstream and upstream transmissions are summarized in Table I. The launched powers of the OLT and ONUs are the minimum values as specified in the baseline proposal [12]. The losses incurred by the fiber, connectors and splitters are also based on specified values.

The optical power budgets for the upstream and downstream links are 22 and 26.2 dB, respectively. The minimum receiver sensitivity required at RX1 and at the OLT are -21 and -29.2 dB, respectively. For the loop-back receiver RX2, the minimum sensitivity required is -21.6 dB, as the optical path traversed by the returned frames is only 2 km.

C. Protocol Description

This subsection describes the proposed EPON protocol, the FULL-RCMA protocol. The basic concept of FULL-RCMA follows the original RCMA protocol [10]. It enhances the RCMA LAN protocol to allow (almost) full channel utilization, even for networks with long links. FULL-RCMA differs from RCMA in the scheduling of data transmissions to minimize the guard times needed between transmissions.

FULL-RCMA is a hybrid between token-passing and contention protocols. It can be viewed as a timed token system, with a target token rotation time of T_{CYCLE}. Once per cycle there is a contention-based "request period," during which sources bid to be first in the token-passing list. The remainder of the cycle is called the "data period." At the end of a request period, the winner of the bidding announces the new token-passing order, including both sources that lost the bidding and sources already in the token-passing list. This has benefits of both worlds: high efficiency during high load from token passing, and low delay during low load from contention.

During the request period, stations contend to submit requests. Short request frames yield low bandwidth wastage, and low chances of collisions. An ONU, which is ready for a data transmission, will be called a *ready* ONU. A ready ONU is required to perform a Request Contention operation for its data transmissions. It first prepares a request frame. The proposed request frame format is depicted in Fig. 3(a). The ONU randomly generates a 7-bit request number and stores

Authorized licensed use limited to: SWINBURNE UNIV OF TECHNOLOGY. Downloaded on January 8, 2009 at 01:52 from IEEE Xplore. Restrictions apply.

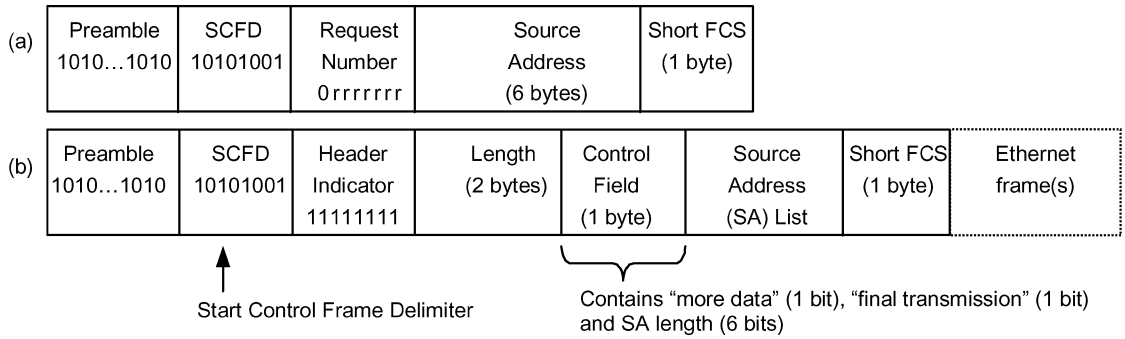

Fig. 3. Frame format. (a) FULL-RCMA request frame. (b) FULL-RCMA header.

it in the request number (RN) field of the request frame. The random distribution used determines the request's priority, as will be described shortly. Its MAC address is also included to identify itself. The request frame ends with an 8-bit short frame check sequence (SFCS) for error detection.

If the channel has been idle for sufficient time, the ready ONU starts a request period by transmitting its request frame immediately. Otherwise, the ready ONU waits until a request period occurs. The start of a request period is announced by the final transmission of the previous data period. The request period has a fixed duration T_{RP} consisting of many slots of length equal to a request frame transmission time. The exact number of slots is a design issue, and is discussed in Section III. (The simpler option of an unslotted request period incurs only a slight performance penalty, as the request period will usually be much shorter than the data period.) After the detection of a request period, a ready ONU broadcasts the request frame in a random time slot uniformly chosen from the request period. The randomness avoids repeated collisions of request transmissions. A collision occurs when two or more transmissions meet at the passive optical splitter causing overlapping of signals and causes all transmissions involved to be unsuccessful.

Throughout the request period, each ONU monitors the echoes from the splitter and sorts the successful requests in decreasing order of RN, using the ONU's MAC address ("source address," SA) to break ties. Note that request collisions at the splitter are detected by all ONUs, and the requests involved are ignored. Each ONU i, whose request did not collide, measures the propagation time R_i between itself and the passive optical splitter. This allows it to determine the times of events at the common reference point, the splitter.

The ONU with the largest RN (with SA tie breaks) is called the *winner*. After the maximum round-trip time T_{RT}, it broadcasts a header [Fig. 3(b)] containing the sorted list of SAs in the order in which the remaining ONUs will transmit. Multiple priorities may be implemented simply by assigning the priority class number to the high-order bits of RN, with large class numbers denoting high priority. The number of SAs in the list is specified in the control field. (Strictly, this can be determined by each ONU, but broadcasting improves reliability in the case of imperfect collision detection.) Immediately following the header, the winner transmits its Ethernet frame. The transmission of a header by the winner marks the start of a data period. The aggregate of a data period and its request period has maximum duration of a predefined "cycle time" denoted T_{CYCLE}. The "cycle time" is designed to limit the channel holding time of each ONU during the data period. This will ensure that real-time services have prompt access to the network, even under heavy load.

The sorted list of SAs in the first header provides information for all other ONUs to schedule their data transmissions. Due to the limited "cycle time," each ONU can only transmit data for a maximum time. Each ONU calculates this time by knowing T_{CYCLE}, T_{RP} and the number of entries in SA list. ONUs are allowed to transmit multiple Ethernet frames in their bursts, as long as they do not exceed the allocated data transmission time. The actual transmission duration is specified in the header [Fig. 3(b)] so that the next ONU knows when it should transmit. If the transmission time is not long enough to clear the local buffer of an ONU, the ONU sets the "more data" bit of the control field of the header. By setting the "more data" bit, the ONU automatically gains access to the next data period without the need for transmitting a request in the next request period.

ONUs other than the winner listen to the header. Each ONU whose MAC address is in the SA list knows the order of transmission. When its turn to transmit comes, it will know when the last bit of the previous transmission will leave the splitter. This is because it knows the length of the transmission (from the header), the time that the first bit arrived, and its own round-trip time (RTT). It can then compute when it can transmit without overlapping the current transmission on the upstream fiber to the OLT and without wasting any time. This pipelining of transmission, similar to that of [3], is the key to achieving high utilization. However, FULL-RCMA does not require the OLT to interleave precisely timed grants with its downstream transmission, as [3] does. The subsequent ONUs must also transmit headers, but these do not repeat the SA list, indicated by a zero SA length field.

The final ONU in the SA list transmits a header with the "final transmission" bit in the control field set indicating that the data period ends when its data transmission is completed. When the "final transmission" bit is detected by a free ONU, it knows that a request period will follow immediately after the data transmission. Free ONUs include those which either suffered a collision when transmitting request frames or became ready during the data period. Only free ONUs are required to contend for data transmissions in the coming request period.

As usual, the free ONUs transmit a request to join the polling list. The winner automatically appends the SAs of those ONUs which had set the "more data" bit in the previous data period to

Authorized licensed use limited to: SWINBURNE UNIV OF TECHNOLOGY. Downloaded on January 8, 2009 at 01:52 from IEEE Xplore. Restrictions apply.

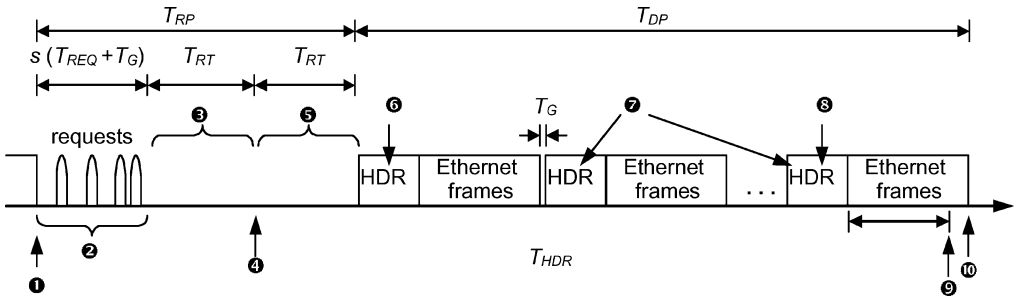

Channel activities observed at the splitter:

❶ End of previous data period, start of a request period
❷ Duration of a request period
❸ Time required for requests to return to all ONUs
❹ All requests returned, winner is decided. The winner starts its transmission
❺ Time required for the winner's transmission to reach the splitter
❻ The first header (HDR) of the data period. It contains transmission orders broadcast in the SA list. Transmission duration for its burst (including header and the Ethernet frames) are also specified
❼ Subsequent header transmissions do not repeat SA list
❽ For the final data transmission, "final transmission" bit must be set indicating the final transmission of the data period
❾ All ONUs detected the end of the data period. ONUs without transmission right can schedule their requests so that the requests appear after ❿

Fig. 4. Illustration of the operation of FULL-RCMA.

the newly formed SA list. Placing the existing ONUs at the end gives the newly joined ONUs higher priority. This guarantees newly joined ONUs prompt access to the network, while maintaining an access delay of no more than one cycle time for those ONUs that requested more bandwidth. Since the latter ONUs need not recontend, the probability of request collision is reduced. If no stations contend, then the ONU which first set the "more data" bit in the previous data period declares itself the winner.

The initialization procedure for FULL-RCMA is simple. As well as at start up, it is invoked to avoid deadlocks if the normal operation of FULL-RCMA is disrupted by, for example, equipment failure. ONUs monitor the channel idle time. During a normal data period, the idle time will remain below a threshold, small compared with T_{RT} and T_{RP}. If this threshold is exceeded, a request period is started. Unlike a request period that is initiated by a "final transmission" bit in the header of a data period, this request period does not have a fixed duration, but continues until an ONU makes a request. This mode is also entered when there are no requests made in a request period following a data period with no ONU setting "more data."

Fig. 4 shows a typical sample of FULL-RCMA activities observed at the common reference point—the splitter. A similar sample for RCMA is given in [10, Fig. 3]. Relative to RCMA, FULL-RCMA achieves a significant reduction in guard time between transmissions by measuring the distance between each ONU and the splitter, and precisely calculating the time of the end of transmission. In contrast, RCMA waits until the channel is idle before the end of transmission is detected. This causes a delay in detecting the end of transmission. As in the carrier sense multiple-access (CSMA) protocol family, this delay increases with the round-trip signal propagation time and thus with the network coverage. This makes RCMA unsuitable for the EPON access networks.

Furthermore, an additional mechanism is proposed to facilitate a bounded cycle time in FULL-RCMA to accommodate applications with tight delay requirement, which is not found in RCMA.

III. Performance Analysis

The simplicity of FULL-RCMA makes it very amenable to analysis. This section shows that, under heavy load, the channel utilization is indeed almost full. An upper bound is then derived for the mean delay incurred in accessing the channel. This is followed by an approximation for the time taken to transmit a burst of data, including both access delay and transmission time. These expressions are used to demonstrate the dependence of the performance on the length of the request period. The analytical results are also used for the optimization of the protocol parameters.

A. Greedy Sources: Peak Channel Utilization

Consider a network with N greedy ONUs wishing to start transmission. A greedy ONU is an ONU that always has a maximum sized Ethernet frame to transmit. In particular, its local buffer is never empty. This assumption models the extreme load condition, and the performance results indicate the upper limit of the network throughput. Under this assumption, the peak utilization of FULL-RCMA is given by

$$U = \frac{T_{\mathrm{DP}} - \Delta}{T_{\mathrm{RP}} + T_{\mathrm{DP}}} \tag{1}$$

where T_{DP} is the duration of a data period, T_{RP} is the duration of a request period, and Δ is the overhead time within the data period. The overhead Δ includes all time within the data period except the transmissions of Ethernet payloads. The peak channel utilization of FULL-RCMA occurs when all greedy ONUs have successfully acquired the channel transmission right, that is, all

Authorized licensed use limited to: SWINBURNE UNIV OF TECHNOLOGY. Downloaded on January 8, 2009 at 01:52 from IEEE Xplore. Restrictions apply.

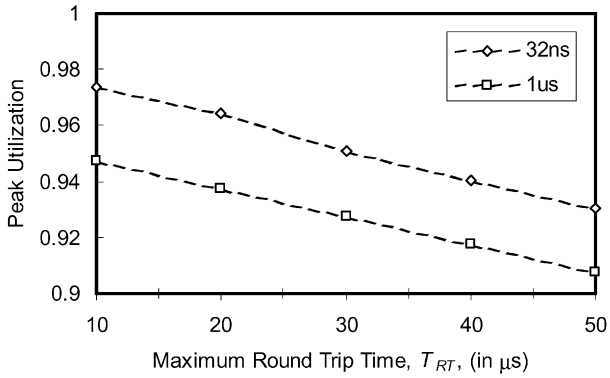

Fig. 5. Peak channel utilization of FULL-RCMA as a function of signal RTT for different guard time settings.

greedy ONUs are already in the polling list. The time for the network to reach this state depends on the time it takes for all ONUs to successfully transmit their requests, which will be dealt with in the next subsection.

Given N greedy ONUs, the header of the very first transmission during a data period contains the SA list for all N ONUs, while the subsequent $N-1$ headers contain no SA list. Thus, an average of one SA is transmitted per header. All greedy ONUs shared the predefined data period equally. They are allowed to burst their Ethernet data frames within their channel holding time. Let $T_{\rm SA}$, $T_{\rm HDR}$, T_H, and $T_{\rm DATA}$ be the respective transmission times for: a single source address field in an SA list, a header (excluding SA list), an Ethernet frame header (including FCS), and a maximum sized Ethernet payload. Let T_G be the guard time between different transmissions. Then

$$T_{\rm DP} = N\left[T_{\rm SA} + T_{\rm HDR} + T_G + n_b\left(T_H + T_{\rm DATA}\right)\right]$$

where

$$n_b = \left\lfloor \frac{T_{\rm CYCLE} - T_{\rm RP} - N\left(T_{\rm HDR} + T_{\rm SA} + T_G\right)}{N(T_H + T_{\rm DATA})} \right\rfloor$$

is the number of Ethernet data frames transmitted by each ONU in a burst during a data period. The overhead time within the data period is then

$$\Delta = T_{\rm DP} - \left(N n_b T_{\rm DATA}\right). \tag{2}$$

Given that a request period can accommodate s slots, the duration of the request period $T_{\rm RP}$ can be expressed in terms of a request frame transmission time $T_{\rm REQ}$, the guard time T_G, and the maximum round-trip time $T_{\rm RT}$, as

$$T_{\rm RP} = s\left(T_{\rm REQ} + T_G\right) + 2T_{\rm RT}. \tag{3}$$

The peak utilization can be determined by substituting (2) and (3) into (1) to get

$$U(N) = \frac{N n_b(N) T_{\rm DATA}}{T_{\rm DP}(N) + s(T_{\rm REQ} + T_G) + 2T_{\rm RT}}. \tag{4}$$

Fig. 5 shows the peak channel utilization of FULL-RCMA as a function of round-trip time $T_{\rm RT}$ between 10 μs and 50 μs, with a "tight" guard time of $T_G = 32$ ns and a "loose" time of

TABLE II
PROTOCOL PARAMETERS USED FOR PEAK UTILIZATION ANALYSIS OF FULL-RCMA

Parameters	Value
Channel data rate, C	1 Gb/s
Request frame transmission time, T_{REQ}	128 ns (16 bytes)
Header transmission time, T_{HDR}	56 ns (7 bytes)
Source address transmission time, T_{SA}	48 ns (6 bytes)
Ethernet header transmission time, T_H	144 ns (18 bytes)
Ethernet payload transmission time, T_{DATA}	12 μs (1500 bytes)
Number of minislots, s	32
Cycle time, T_{CYCLE}	2 ms

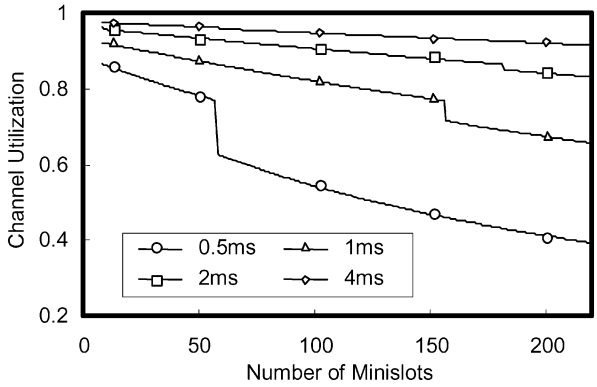

Fig. 6. Channel utilization versus number of minislots for $T_{\rm CYCLE}$ between 0.5–4 ms.

$T_G = 1$ μs [14], [15]. Other protocol parameters used in this study are given in Table II.

The maximum RTT depends on the maximum coverage of the FULL-RCMA splitter. It is independent of the distance between the splitter and the OLT since the OLT does not use FULL-RCMA to perform transmissions. Hence, the placement of the OLT relative to the splitter is not constrained by timing issues, but only be the need for the OLT to be able to detect signals transmitted by the ONUs. With propagation delay of 5 μs/km, a RTT of $T_{\rm RT} = 10$ μs is equivalent to a network coverage of 1-km radius around the splitter, assuming that the splitter is located in the center of all ONUs. Clearly, both guard time settings give reasonably high-peak utilization, particularly, for 32 ns (or 32-bit time) guard time setting. The difference of peak utilization between the two settings is only about 2%. This indicates that the higher precision transceivers required for 32 ns guard times may not be justified on efficiency grounds.

For a guard time of $T_G = 1$ μs and a network coverage of 1-km radius around the splitter, Fig. 6 shows the peak utilization as a function of s, the number of request slots, for several values of $T_{\rm CYCLE}$. The request period, $T_{\rm RP}$, increases steadily with s, causing the steady drop in utilization, but there are also discrete drops in the utilization in Fig. 6. These are due to the quantization of n_b to integers. Once $T_{\rm DP}+T_{\rm RP} > T_{\rm CYCLE}$, n_b decreases by one to restore the condition $T_{\rm DP}+T_{\rm RP} \le T_{\rm CYCLE}$. This has a greater relative impact on the utilization when n_b is smaller.

B. Greedy Sources: Time to Join

This section deals with the time for N greedy ONUs to join the network. Specifically, it calculates how long after the start of a request period they will all be in the polling list. This is

Authorized licensed use limited to: SWINBURNE UNIV OF TECHNOLOGY. Downloaded on January 8, 2009 at 01:52 from IEEE Xplore. Restrictions apply.

bounded above by J_n, the time from the simultaneous arrival of n ONUs until the end of the first data period in which all n ONUs are in the list. For simplicity, only the case of a slotted request period will be considered. Set $J_0 = 0$. For $n > 1$, the value of J_n depends on the number of ONUs k, which successfully reserve a slot during the request period. The time required will then be the time for the current cycle $T_{\rm RP} + T_{\rm DP}$ plus the time for the remaining $n - k$ ONUs to join. Let B be the event that there is already at least one (greedy) source in the list. Then

$$E[J_n|B] = \sum_{k=0}^{n} (T_{\rm RP} + T_{\rm DP} + E[J_{n-k}|B])P(k; n, s) \quad (5)$$

where $P(k; n, s)$ is the probability of k successful requests when n ONUs compete for s request slots. For computational purposes, this implicit equation can be rewritten as (6), shown at the bottom of the page. Subsequent implicit equations can also be rewritten similarly.

An efficient recurrence relation can be used to find $P(k; n, s)$. Let $P_{n,s}(i, j, k)$ be the probability of there being i slots with no requests, j slots with two or more requests, and k slots with exactly one request. Then, $P(k; n, s) = \sum_{i+j=n-k} P_{n,s}(i, j, k)$ and

$$P_{n+1,s}(i, j, k) = \frac{j}{s} P_{n,s}(i, j, k) + \frac{i+1}{s} P_{n,s}(i+1, j, k-1) + \frac{k+1}{s} P_{n,s}(i, j-1, k+1) \quad (7)$$

for $i, j, k, n \geq 0$, with the initial conditions zero except for

$$P_{0,s}(1, 0, 0) = 1. \quad (8)$$

If the network is initially empty and there are no successful requests, then the current cycle will only have length $T_{\rm RP}$ instead of $T_{\rm RP} + T_{\rm DP}$. Thus

$$E[J_N|\overline{B}] = P(0; n, s)(T_{\rm RP} + E[J_N|\overline{B}]) + \sum_{k=1}^{n} (T_{\rm RP} + T_{\rm DP} + E[J_{n-k}|B])P(k; n, s). \quad (9)$$

The value in (9) is plotted in Fig. 7 for the same conditions as Fig. 6. For fewer than around $s = 30$ request slots, the delay is large due to the high probability of requests colliding, causing ONUs to have to wait multiple cycles. For s above 50 or so, the delay is dominated by the length of the cycle time, and increases with s, except at the points where n_b is discontinuous.

C. Real-Time Sources: Expected Delay in a Worst Case Scenario

Another important scenario is a network transmitting real-time data at regular intervals, such as video or voice frames. Consider N sources producing single packets at equal intervals of P, assumed to be larger than the cycle time. In a stable network with no other traffic, the work arriving at a given instant will be cleared within time P, and so the highest delay which could be experienced would occur if all users arrive simultaneously. What, then, is the expected total transmission time, excluding the time taken to join the polling list, for a burst arrival of R packets, each of duration $T_{pk} = T_H + T_{\rm DATA}$? Again, this can be calculated in terms of a two-dimensional recurrence relation.

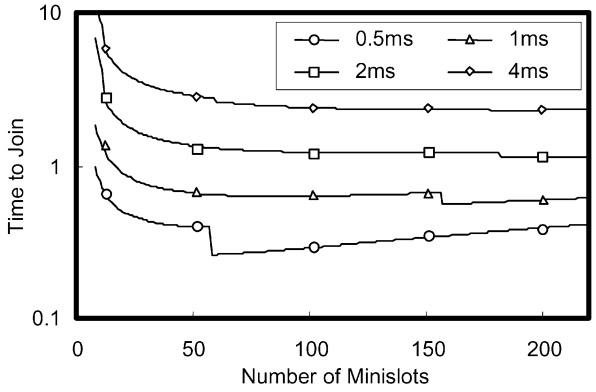

Fig. 7. Time (milliseconds) to join versus number of minislots for $T_{\rm CYCLE}$ between 0.5–4 ms.

Recall that at most Nn_b packets can be transmitted within the cycle time, which may be less than the number of request slots, s. Thus, stations may join the token list without receiving a chance to transmit in that cycle. At the start of a request period, there will in general be r new sources waiting to join the polling list and a backlog of b sources who have made successful requests to join the list, but not yet had a chance to transmit. Let $C(r, b)$ be the time to clear this batch. Once all the sources have joined the polling list, the time to clear the backlog is the sum of the actual time to transmit the backlogged packets (bT_{pk}) and the time of the $\lceil b/Nn_b \rceil$ reservation periods

$$C(0, b) = bT_{pk} + \left\lceil \frac{b}{Nn_b} \right\rceil T_{\rm RP}. \quad (10)$$

While there are still $r \neq 0$ sources wishing to join, the expected time to clearance at the start of each request period obeys a recurrence relation. This splits into two cases depending on whether or not the length of the polling list, after the request period, exceeds Nn_b sources. If there are $k \leq Nn_b - b$ successful requests, then there will be $k + b \leq Nn_b$ sources able to transmit, and they will all be transmitted in the current cycle. This will take time $T_{\rm RP} + (k+b)T_{pk}$, and leave $r - k$ stations to be cleared in future cycles. If there are $k > Nn_b - b$ successful requests, then, Nn_b will be able to transmit, and the rest will be backlogged. Weighting these outcomes by their probabilities of occurrence gives (11), shown at the bottom of the next page.

The expected time to clear R sources that arrive when there is no backlog is then $E[C(R, 0)]$. Note that this delay decreases as

$$E[J_n|B] = \frac{(T_{\rm RP} + T_{\rm DP})P(0; n, s) + \sum_{k=1}^{n} (T_{\rm RP} + T_{\rm DP} + E[J_{n-k}|B])P(k; n, s)}{1 - P(0; n, s)} \quad (6)$$

Authorized licensed use limited to: SWINBURNE UNIV OF TECHNOLOGY. Downloaded on January 8, 2009 at 01:52 from IEEE Xplore. Restrictions apply.

n_b increases, while the delay of (9) increases as $T_{\rm DP}$ increases. Thus, networks carrying both real-time and greedy sources must compromise on the cycle time, as described next.

D. Mixed Sources: Delay in the Presence of Greedy Sources

Consider n real-time sources simultaneously wishing to transmit amounts of data l_i, $i = 1,\ldots,n$, while g greedy sources are transmitting. This section will derive an expression for the mean delay each real-time source experiences. This delay will be approximated as the sum of two parts: the mean time for a source to join the polling list, and the mean remaining delay given all n sources have simultaneously been admitted.

Given n sources wishing to join the polling list, the mean time between the start of the next request period and the end of the data period in which a source is admitted can be derived analogously to (5). It is

$$E[M_n] = \sum_{k=0}^{n} \left(T_{\rm RP} + T_{\rm DP} + \frac{n-k}{n} E[M_{n-k}] \right) P(k;n,s). \tag{12}$$

On average, the time between the sources becoming ready to transmit and the start of the next request period is $(T_{\rm RP} + T_{\rm DP})/2$. Moreover, the sources can start transmitting at the start of the data period of the cycle in which they join, rather than at the end of the data period. Thus, the total expected interval between the time one of the n sources becoming ready to send data and the time it can start transmitting is $E[M_n] + (T_{\rm RP} - T_{\rm DP})/2$.

To calculate the mean time taken for a source to transmit its data once it has joined the polling list, assume without loss of generality that $l_i \geq l_{i+1}$ for all i, with $l_{n+1} = 0$. Between the time that source i is cleared and source $i+1$ is cleared, there will be $g+i$ sources sharing the available bandwidth, with a total utilization $U(g+i)$ given by (4). The total time for l_1 to clear is then

$$E[M_n] + \frac{(T_{\rm RP} - T_{\rm DP})}{2} + \sum_{i=1}^{n} \frac{(g+i)(l_i - l_{i+1})}{U(g+i)C}$$

where $C = 10^9$ b/s is the capacity of the link.

Fig. 8 shows these results for $g = 4$, $n = 12$ and $l_i = 120\,000$ bits (ten packets), for $i = 1,\ldots,n$. This shows that the minimum total time is achieved by having a fast cycle time, with a small number of request slots per cycle. Having a fast cycle and, hence, more frequent request periods, increases the overhead introduced by having excessive request slots per cycle. However, for up to $s = 50$ request slots, this is more than outweighed by the reduction in time taken to join the polling list.

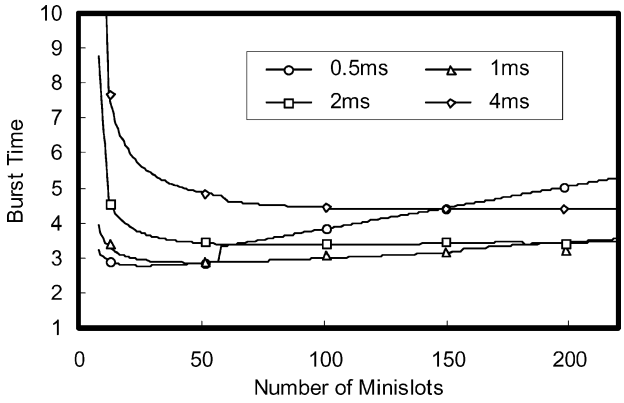

Fig. 8. Burst time (milliseconds) versus number of minislots for $T_{\rm CYCLE}$ between 0.5–4 ms.

E. Parameter Selection

A simplified model provides useful insight into the optimal choice of target cycle time T_C and the number of request slots s for the scenario of the previous section. The total time required to transmit a burst of data can be broken into three components: the time to join T_j, the actual transmission time T_X, and the protocol overheads T_p. Since the actual transmission time T_X is independent of the protocol parameters, the aim is to minimize the sum of the other two components. The average time to join T_j is the product of T_C and the expected number of cycles required to join, which is a decreasing function of s : $T_j = f(s)T_C$. The protocol overhead is incurred T_X/T_C times, once for each cycle through the polling list, giving a total protocol overhead of $T_p = g(s)T_X/T_C$. Combining these, $T_j + T_p$ is minimized with respect to T_C when

$$f(s)T_C^2 = g(s)T_X. \tag{13}$$

The optimal cycle time is proportional to the square root of the average amount of data per burst. In practice, a fixed cycle time will generally be used, since T_X cannot be known in advance. This study uses a value of 2 ms, which is chosen as a suitable value for real time services, being an order of magnitude less than the 20-ms delay, typically incurred in voice coding. The choice of a 1-μs guard time has been discussed previously. From Fig. 8, a suitable value is around 32.

F. Performance Comparison

A performance comparison between FULL-RCMA, RCMA and IPACT is presented in Fig. 9. We compare the peak channel utilization of these protocols for a range of numbers of greedy

$$\begin{aligned} E[C(r,b)] = & \sum_{k=0}^{\min(Nn_b-b,r)} P(k;r,s)(T_{\rm RP} + (k+b)T_{pk} + E[C(r-k,0)]) \\ & + \sum_{k=Nn_b-b+1}^{r} P(k;r,s)(T_{\rm RP} + Nn_bT_{pk} + E[C(r-k,k+b-Nn_b)]) \end{aligned} \tag{11}$$

Authorized licensed use limited to: SWINBURNE UNIV OF TECHNOLOGY. Downloaded on January 8, 2009 at 01:52 from IEEE Xplore. Restrictions apply.

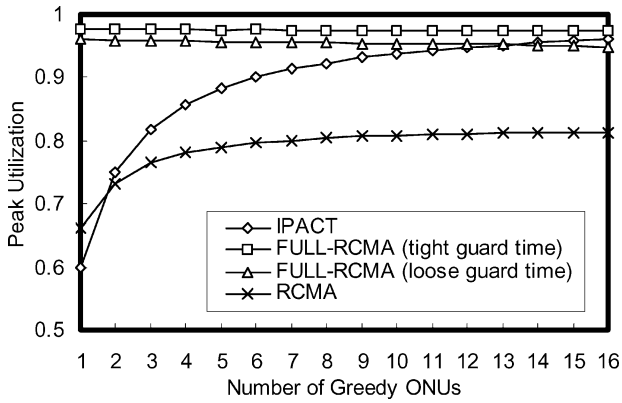

Fig. 9. Performance comparison of FULL-RCMA, RCMA, and IPACT.

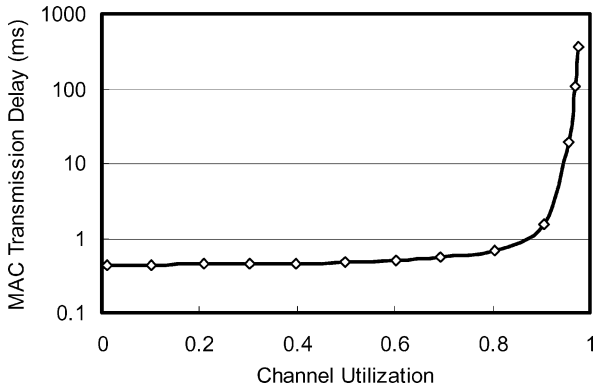

Fig. 10. Mean packet transmission delay versus channel utilization of FULL-RCMA for 16 Pareto ON/OFF sources.

ONUs. IPACT is based on TDMA with the following peak utilization [3]:

$$U_{\text{IPACT}} = \frac{NT_d}{NT_d + N_t T_g} \tag{14}$$

where T_d is the maximum data transmission time for each ONU, T_g is the guard time between two transmissions, and N_t is the total number of ONUs in the EPON. The suggested values for these parameters are given in [3], specifically, $T_d = 0.12$ ms (or 120-k bit time), $T_g = 5\ \mu$s, and $N_t = 16$.

To apply EPON configuration to RCMA that is originally designed for a LAN, two minor modifications are made to the RCMA operation, namely: 1) each LAN station, when successfully made a request, transmits up to 0.12 ms in the following data period and 2) the distance between a LAN station and the RCMA splitter is set to 1 km. The results presented here are computed based on the analysis of the RCMA given in [10].

With the peak channel utilization for FULL-RCMA given in Section III, a comparison of peak channel utilization of FULL-RCMA, RCMA, and IPACT is given in Fig. 9. We see significant improvement in performance of FULL-RCMA over RCMA. It is mainly due to the enhancements made in FULL-RCMA to reduce the guard time between transmissions.

The results also show that the performance of FULL-RCMA is relatively insensitive to the number of greedy ONUs and FULL-RCMA performs better than IPACT in most cases. IPACT inherits the property of TDMA that it achieves higher utilization as the number of greedy ONUs increases. The peak utilization increases from 60% (that is, better performance at heavy loading). As oppose to IPACT, the increase in the number of greedy ONUs causes a slight drop in FULL-RCMA performance, this is because more greedy ONU's results in more overheads in guard time between transmissions. However, the enhancements made in FULL-RCMA have reduced these overheads, for example, FULL-RCMA with tight guard time continues to perform better than IPACT even for the case of 16 greedy ONUs.

IV. Simulation Study

This section studies the performance of FULL-RCMA under realistic traffic models via computer simulation. In particular, Pareto ON/OFF sources are used to model aggregated data traffic, and constant bit rate (CBR) sources are considered for real-time multimedia traffic. We study the delay performance of two cases: a network with nonreal-time (data) traffic only, and a network with mixture of data and real-time traffic.

A. Pareto ON/OFF Sources

Each ONU is modeled as an ON/OFF source. The duration of the on and the off periods are Pareto distributed. To capture the long range dependent property of the data traffic, the shape parameter of the Pareto distribution function is set to 1.4, which will produce traffic with a Hurst parameter of 0.8. During an on period, a source generates traffic into its local buffer at a data rate of 100 Mb/s. The size of each local buffer is set to 10 Mbytes. The choice of Hurst parameter is based on the study in [17]. This traffic assumption models the situation where the bandwidth of an ONU is shared by a number of users connected by a LAN attached to the ONU. A network of radius 1 km around the splitter and 1-μs guard time are considered, with other protocol parameters given in Table II.

Fig. 10 shows the mean packet transmission delay as a function of channel utilization. The delay is measured from the time when the first bit is generated until the last bit has arrived at the OLT, which is located 20 km away from the splitter. The offered load of the network is controlled by adjusting the Pareto off period of all ONUs. The delay curve shows that even under heavy load, the delay remains low. It starts to increase sharply when the channel utilization is closed to 100%. This result confirms the very high utilization achievement of FULL-RCMA even under realistic traffic. In most load range, the mean packet transmission delay remains below 1 ms. This short delay indicates the high efficiency of FULL-RCMA.

B. Pareto ON/OFF and Real-Time Sources

In this section, we study the delay performance of real-time sources. Consider a network of two types of ONU sources: Pareto ON/OFF sources and real-time sources. Pareto ON/OFF sources follow the model described in the previous subsection. Each source represents a collection of end users connected by a LAN. Real-time sources are modeled as CBR sources, where each real-time source starts at a randomly chosen time and continue to transmit with constant ON/OFF duration. Each real-time ONU source represents a user generating traffic at a CBR. With

Authorized licensed use limited to: SWINBURNE UNIV OF TECHNOLOGY. Downloaded on January 8, 2009 at 01:52 from IEEE Xplore. Restrictions apply.

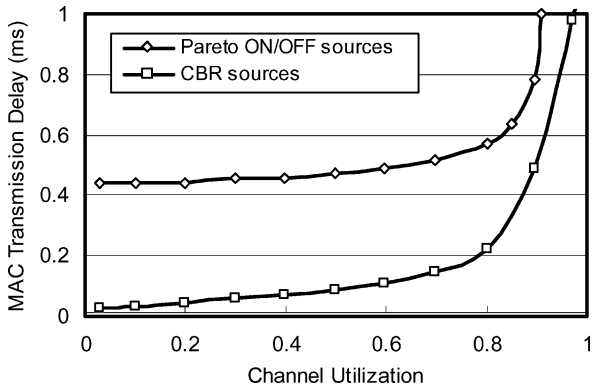

Fig. 11. Mean packet transmission delay versus channel utilization of FULL-RCMA for 12 Pareto ON/OFF and four CBR sources.

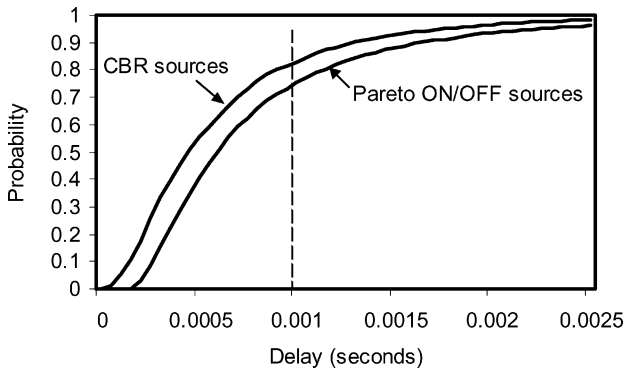

Fig. 12. Cumulative distribution of packet transmission delay for 12 Pareto ON/OFF and four CBR sources at channel utilization of 0.9.

this model, we are able to exclude the queueing delay at ONUs, which is related to the queue priority scheme implemented at the ONU rather than the performance of FULL-RCMA. This model is similar to the situation where the real-time traffic is always served before any other traffic at the ONU.

In additional to the protocol parameters listed in Table II, we consider a network of 16 ONUs of which four are real-time sources and 12 are Pareto ON/OFF sources. The OLT is located 20 km away from the splitter. As in the previous simulation experiment, the shape parameter of the Pareto distribution function is set to 1.4. The rate at which data is generation during an ON period is 100 Mb/s. The size of the local buffer of each ONU is limited to 10 Mbytes. The real-time sources generate 200 bits of information every 20 ms, giving a data rate of 10 kb/s.

Fig. 11 presents the average delay experienced by a Pareto ON/OFF source and a real-time CBR source. The traffic load of the network is varied by adjusting the OFF duration of the 12 Pareto ON/OFF sources. The CBR sources experience lower delay because the packets are generally small; the average delay of CBR packets remains below 1 ms until the load is extremely high.

To illustrate the ability of FULL-RCMA to carry real-time multimedia traffic, Fig. 12 plots the cumulative delay distributions of the two ONU types. We consider heavy load conditions where the FULL-RCMA protocol operates at channel utilization of 0.9. The figure shows that over 80% of CBR packets are transmitted successfully from the real-time ONUs to the OLT within 1 ms. Just below 75% of data packets are transmitted from the ONUs to the OLT within 1 ms. Furthermore, over 90% of packets of both types are delivered from ONUs to OLT within 2 ms. These results compare favorably with those reported for the algorithm of [9]. The low delay variance indicated in the figure allows FULL-RCMA to carry multimedia traffic with high quality-of-service.

V. Conclusion

We have introduced a new EPON solution, using a new MAC protocol named FULL-RCMA. We studied the physical layer implementation and MAC layer protocol performance to illustrate the feasibility and benefit of our solution. The optical link budget analyses of the proposed EPON architecture have shown the possibility of the practical deployment of our EPON solution using currently available optical components.

We have performed a detailed analysis on the performance of the FULL-RCMA MAC protocol for our proposed EPON solution. The protocol has been found to be very efficient. It can operate at over 90% channel utilization. We further evaluated the effect of several important protocol parameters on the performance in order to achieve an optimum protocol operation given a particular network configuration. In addition, we also studied the performance of FULL-RCMA carrying multimedia traffic, specifically CBR traffic. The study indicates that delivery of multimedia traffic with a high QoS can be achieved with our EPON solution.

References

[1] H. Lee, D. Lee, and C. Oh, "A MAC scheme with double-side scheduling for ATM-based PON," *IEICE T. Commun.*, vol. E84B, pp. 1690–1693, 2003.

[2] G. Kramer and G. Pesavento, "Ethernet passive optical network (EPON): Building a next-generation optical access network," *IEEE Commun. Mag.*, pp. 66–73, Feb. 2002.

[3] G. Kramer, B. Mukherjee, and G. Pesavento, "IPACT: A dynamic protocol for an Ethernet PON (EPON)," *IEEE Commun. Mag.*, pp. 74–80, Feb. 2002.

[4] "MPCP – State of the Art" PDF Presentation (2002, Jan.). [Online]. Available: http://www.ieee802.org/802/3/efm/public/jan02/maislos_1_0102.pdf

[5] G. Kramer, B. Mukherjee, and G. Pesavento, "Ethernet PON (ePON): Design and analysis of an optical access network," *Photonic Network Commun.*, vol. 3, no. 3, pp. 307–319, July 2001.

[6] M. Ma, Y. Zhu, and T. H. Cheng, "A bandwidth guaranteed polling MAC protocol for Ethernet passive optical networks," in *Proc. IEEE INFOCOM*, vol. 1, Mar. 2003, pp. 2–31.

[7] F.-T. An, Y. L. Hsueh, K. S. Kim, I. M. White, and L. G. Kazovsky, "A new dynamic bandwidth allocation protocol with quality of service in Ethernet-based passive optical networks," in *Proc. IASTED Wireless Optical Communications Conf.*, July 2003, pp. 165–169.

[8] H.-J. Byun, J.-M. Nho, and J.-T. Lim, "Dynamic bandwidth allocation algorithm in Ethernet passive optical networks," *IEEE Electron. Lett.*, vol. 39, pp. 1001–1002, June 2003.

[9] C. M. Assi, Y. Ye, S. Dixit, and M. A. Ali, "Dynamic bandwidth allocation for quality-of-service over Ethernet PONs," *IEEE J. Select. Areas Commun.*, vol. 21, pp. 1467–1477, Nov. 2003.

[10] C. H. Foh and M. Zukerman, "A novel and simple MAC protocol for high-speed passive optical LANs," in *Proc. Networking 2002*, Pisa, Italy, 2002, pp. 467–478.

[11] "Single or dual fiber for 100 Mb/s over SMF?" PDF Presentation (2002, Jan.). [Online]. Available: http://www.ieee802.org/3/efm/public/jan02/mickelsson_2_0102.pdf

[12] "P2MP PMD baseline" PDF Presentation (2002, Mar.). [Online]. Available: http://www.ieee802.org/3/efm/baseline/effenberger_ 1_0302.pdf

[13] Y. Ota and R. G. Swartz, "Burst-mode compatible optical receiver with a large dynamic range," *J. Lightwave Technol.*, vol. 8, pp. 1897–1903, Dec. 1990.

Authorized licensed use limited to: SWINBURNE UNIV OF TECHNOLOGY. Downloaded on January 8, 2009 at 01:52 from IEEE Xplore. Restrictions apply.

[14] "Guard Band Requirements," PDF Presentation (2002, May). [Online]. Available: http://grouper.ieee.org/groups/802/3/efm/public/may02/maislos_2_0502.pdf
[15] "PON PMD Timing," PDF Presentation (2003, Jan.). [Online]. Available: http://www.ieee.802.org/3/efm/public/jan03/optics/effenberger_optics_1_0103.pdf
[16] Y. Ota, R. G. Swartz, and V. D. Archer III, "DC-1 Gb/s burst-mode compatible receiver for optical bus applications," *J. Lightwave Technol.*, vol. 10, pp. 244–249, Feb. 1992.
[17] W. E. Leland, M. S. Taqqu, W. Willinger, and D. V. Wilson, "On the self-similar nature of Ethernet traffic (extended version)," *IEEE/ACM Trans. Networking*, vol. 2, pp. 1–15, Feb. 1994.

Chuan Heng Foh (S'00–M'03) received the B.S. degree in electronic engineering from Fu Jen Catholic University, Taipei Hsien, Taiwan, R.O.C., in 1992, the M.S. degree from Monash University, Victoria, Australia, in 1999, and the Ph.D. degree from the University of Melbourne, Melbourne, Australia, in 2002.

From July 2002 to December 2002, he was a Lecturer at Monash University. He is now an Assistant Professor with the School of Computer Engineering, Nanyang Technological University, Singapore. His research interests include protocol design and performance analysis of mobile wireless and optical networks.

Lachlan Andrew (M'97) received the B.Sc. degree in computer science, the B.E. degree in electrical engineering, and the Ph.D. degree in engineering from the University of Melbourne, Melbourne, Australia, in 1992, 1993, and 1996, respectively.

He is a Research Fellow in the Department of Electrical and Electronic Engineering, University of Melbourne. His research interests include performance analysis and resource allocation in optical and wireless communication networks. Specific interests are optical burst switching, flow control, and ad hoc networks.

Dr. Andrew is a member of the Institution of Electrical Engineers, U.K.

Elaine Wong (S'98–M'02) received the B.E. degree (first-class honors) and the Ph.D. degree in electrical and electronic engineering from the University of Melbourne, Melbourne, Australia, in 1998 and 2002, respectively. Her Ph.D. dissertation was on the topic of collision avoidance in all-optical wavelength-division-multiplexing (WDM) packet networks.

Since the completion of her Ph.D. degree, she has been with the University of Melbourne and the Australian Photonics Cooperative Research Centre's Photonics Research Laboratory. Her research interests include optical signal monitoring technologies for optical networks, and multiple-access protocols and architectures for WDM networks.

Dr. Wong is a recipient of the IEEE Laser and Electro-Optics Society (LEOS) Graduate Student Fellowship Award 2001.

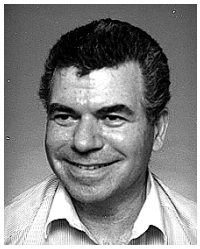

Moshe Zukerman (M'87–SM'91) received the B.Sc. degree in industrial engineering and management and the M.Sc. degree in operation research from Technion—Israel Institute of Technology, Haifa, and the Ph.D. degree in electrical engineering from the University of California, Los Angeles (UCLA), in 1985.

He was an independent consultant with IRI Corporation, Los Angeles, CA, and a Postdoctoral Fellow at UCLA from 1985 to 1986. From 1986 to 1997, he was with Telstra Research Laboratories (TRL), Clayton, Australia, first as a Research Engineer and from 1988 to 1997, as a Project Leader. In 1997, he joined the University of Melbourne, where he was responsible for promoting and expanding telecommunications research and teaching in the Electrical and Electronic Engineering Department. Since 1990, he has also taught and supervised graduate students at Monash University, Victoria, Australia. He has authored over 200 publications in scientific journals and conference proceedings and has been awarded several national and international patents.

Dr. Zukermann was the recipient of the Telstra Research Laboratories Outstanding Achievement Award in 1990. He also served as a Guest Editor of the IEEE JOURNAL ON SELECTED AREAS IN COMMUNICATIONS for two issues: Future Voice Technologies and Analysis and Synthesis of MAC Protocols. Presently, he is serving on the Editorial Board of the IEEE/ACM TRANSACTIONS ON NETWORKING, the *International Journal of Communication Systems*, *Computer Networks*, and as a Wireless Communications Series Editor for the IEEE *Communications Magazine*. He served on the Editorial Board of the *Australian Telecommunications Research Journal* from 1991 to 1996. He submitted contributions to and represented Australia at several ITU-T/CCITT standards meetings.

Authorized licensed use limited to: SWINBURNE UNIV OF TECHNOLOGY. Downloaded on January 8, 2009 at 01:52 from IEEE Xplore. Restrictions apply.